Development 135, 3511-3519 (2008) doi:10.1242/dev.027144

Functional importance of evolutionally conserved Tbx6 binding sites in the presomitic mesoderm-specific enhancer of *Mesp2*

Yukuto Yasuhiko[1,*], Satoshi Kitajima[1], Yu Takahashi[1], Masayuki Oginuma[2], Harumi Kagiwada[3], Jun Kanno[1] and Yumiko Saga[2,*]

The T-box transcription factor Tbx6 controls the expression of *Mesp2*, which encodes a basic helix-loop-helix transcription factor that has crucial roles in somitogenesis. In cultured cells, Tbx6 binding to the *Mesp2* enhancer region is essential for the activation of *Mesp2* by Notch signaling. However, it is not known whether this binding is required in vivo. Here we report that an *Mesp2* enhancer knockout mouse bearing mutations in two crucial Tbx6 binding sites does not express *Mesp2* in the presomitic mesoderm. This absence leads to impaired skeletal segmentation identical to that reported for *Mesp2*-null mice, indicating that these Tbx6 binding sites are indispensable for *Mesp2* expression. T-box binding to the consensus sequences in the *Mesp2* upstream region was confirmed by chromatin immunoprecipitation assays. Further enhancer analyses indicated that the number and spatial organization of the T-box binding sites are critical for initiating *Mesp2* transcription via Notch signaling. We also generated a knock-in mouse in which the endogenous *Mesp2* enhancer was replaced by the core enhancer of medaka *mespb*, an ortholog of mouse *Mesp2.* The homozygous enhancer knock-in mouse was viable and showed normal skeletal segmentation, indicating that the medaka *mespb* enhancer functionally replaced the mouse *Mesp2* enhancer. These results demonstrate that there is significant evolutionary conservation of Mesp regulatory mechanisms between fish and mice.

KEY WORDS: T-box transcription factor, Enhancer, Targeted disruption, Somitogenesis

INTRODUCTION

Somitogenesis is an important morphogenic process that generates metameric structures in vertebrates, including vertebra, muscles and motoneurons. The segmental boundary of each somite forms at the anterior end of the presomitic mesoderm (PSM) or unsegmented paraxial mesoderm, which are supplied from the primitive streak or tailbud at a later stage of development (Saga and Takeda, 2001). This process proceeds through the interaction of a number of signaling cascades, including Notch, Wnt and Fgf (Delfini et al., 2005; Dunty et al., 2008; Galceran et al., 2004; Hofmann et al., 2004; Moreno and Kintner, 2004; Takahashi et al., 2000). Thus, somitogenesis could be a very useful model system in which to study the interactions among the various signaling cascades that facilitate periodic pattern formation.

The basic helix-loop-helix transcription factor Mesp2 plays a crucial role in both somite segment border formation and in the establishment of the rostrocaudal patterning of each somite (Saga et al., 1997). *Mesp2* shows dynamic and periodic expression in the anterior PSM. This expression pattern defines the positioning of the newly forming somite by suppressing Notch signaling, in part through the activation of lunatic fringe (*Lfng*) (Morimoto et al., 2005). Genetic analyses have revealed that *Mesp2* expression is itself controlled by Notch signaling, indicating the existence of complicated feedback circuitry (Takahashi et al., 2003; Takahashi et al., 2000). We have previously identified the minimal PSM-specific *Mesp2* enhancer (denoted P2PSME) that is sufficient to reproduce the normal *Mesp2* expression pattern in transgenic animals (Haraguchi et al., 2001). We have also demonstrated that the T-box transcriptional regulator Tbx6 directly binds to P2PSME and is essential for P2PSME activity (Yasuhiko et al., 2006). We also showed that Notch signaling strongly enhanced *Mesp2* activation via Tbx6 and we identified the sequences that are important for this enhancement using an in vitro reporter assay (Yasuhiko et al., 2006). However, the question of whether P2PSME is indispensable for *Mesp2* expression during somitogenesis remained to be addressed. Because of differences in the expression patterns of *Mesp2* and Tbx6 – Tbx6 is expressed throughout the PSM and tailbud (Chapman et al., 1996; White and Chapman, 2005) whereas *Mesp2* expression is observed only in the anterior PSM (Saga et al., 1997) – another open question was whether Tbx6 actually binds to P2PSME.

The evolutionary aspect of this system is also noteworthy. We previously identified the *mespb* PSM-specific enhancer in the teleost fish medaka, and reported that the mutation of two T-box binding sites therein diminished its PSM-specific enhancer activity in transgenic embryos (Terasaki et al., 2006). However, definitive evidence as to whether the T-box-factor-dependent regulation is a conserved mechanism among vertebrates remains elusive.

In this study, we established *Mesp2* enhancer knockout mice and confirmed that Tbx6 binding sequences are essential for *Mesp2* expression. The in vivo association of Tbx6 with P2PSME was confirmed in chromatin immunoprecipitation assays, and reporter assays further showed that the number and spatial organization of Tbx6 binding sites are important for P2PSME activity. Furthermore, using a knock-in mouse that harbors the medaka *mespb* enhancer in place of the mouse *Mesp2* enhancer, we show that the T-box-factor-dependent regulation of the Mesp gene is evolutionally conserved between fish and mice.

[1]Division of Cellular and Molecular Toxicology, National Institute of Health Sciences, 1-18-1 Kamiyoga, Setagaya-ku, Tokyo 158-8501, Japan. [2]Division of Mammalian Development, National Institute of Genetics, 1111 Yata, Mishima, Shizuoka 411-8540, Japan. [3]Research Institute for Cell Engineering, National Institute of Advanced Industrial Science and Technology, 3-11-46 Nakoji, Amagasaki, Hyogo 661-0974 Japan.

*Authors for correspondence (e-mails: yasuhiko@nihs.go.jp; ysaga@lab.nig.ac.jp)

Accepted 8 September 2008

MATERIALS AND METHODS

Site-directed mutagenesis

Site-directed mutagenesis of each Tbx6 binding site was performed using previously reported PCR-based procedures (Yasuhiko et al., 2006) with the following primers (mutated nucleotides in lower case): mB1, 5′-CCTTCGAGGGGTCAGAATCgAtAtCTCTGCAAATGGGCCCGCTTT-3′; mB2, 5′-CCTTCGAGaGtaCtGAATCCACACCTCTGCAAATGG-GCCCGCTTT-3′; mD, 5′-AACCTGGCAGGGGACCACCTCgCgaCTT-TAGTCCAGATAAAAGCT-3′; mG, 5′-CTGGGCTCTGTGGGTTTTG-AattCTCTCTGCAACCTGGCA-3′. The mutated Tbx6 binding sites are indicated for each construct, such that P2EmB1D represents a P2PSME containing both mB1 and mD.

Gene targeting

For targeted disruption of P2PSME, a 356-bp DNA fragment containing mutated Site B and Site D was generated by PCR using primers mB1 and mD. As a negative control, the wild-type P2PSME fragment was also generated by PCR. To construct the targeting vectors, a floxed PGK-neoR selection marker cassette was inserted between a 6-kb long arm and the 356-bp DNA fragment with or without mutations (Fig. 1A). The region corresponding to *Mesp2* exon 1, intron 1 and a part of exon 2 served as the short homology arm. The targeting vector was introduced into mouse ES cells (strain TT2) by electroporation. Resulting G418-resistant ES clones were characterized by PCR using primers: Fesneo, 5′-CGCCTTCT-ATCGCCTTCTTGACGAG-3′ and RP213, 5′-CAGGACAGCCACT-GAGCTGCAGGCCTGA-3′. Southern blots were performed to confirm homologous recombination. Positive ES clones were then aggregated with 8-cell stage ICR mouse embryos in order to produce chimeric mice. The ES selection marker PGK-neoR was removed by crossing the chimeric mice with CAG-Cre mice, which express Cre recombinase ubiquitously. The resulting mouse strains, with insertions of either mutated P2PSME or wild-type P2PSME, were designated P2EmB1D or P2EmCont, respectively. Although the knockout mice were established using an ES cell line (TT2) obtained from a C57BL/6 × CBA cross (Yagi et al., 1993), mice were maintained in an ICR background unless otherwise stated.

Skeletal preparation

Embryonic day 17.5 (E17.5) mouse embryos were obtained by crossing the mutants of interest. Embryos were then fixed with 90% ethanol. For genotyping, PCR was performed using a piece of embryonic liver digested with proteinase K (Roche). Alcian Blue and Alizarin Red staining were performed as described (Saga et al., 1997; Takahashi et al., 2000).

Generation of anti-Tbx6 antibody

His-tagged fragments of Tbx6 protein (N-terminal antigen, amino acids 2-78; internal antigen, amino acids 311-408) (White and Chapman, 2005) were produced using the pET system (Novagen) and *Escherichia coli* Rosetta-gamiB (Novagen) as a host strain. The Tbx6 fragments were extracted from bacterial culture using the MagneHis system (Promega), purified by thrombin digestion to remove the His-tag, followed by affinity column purification (Novagen) and dialysis using a semipermeable membrane cassette (Pierce). Rabbits (two animals for each antigen) were immunized with the purified Tbx6 fragments and processed for antibody purification following the standard procedures of Hokudo Bio (Abuta, Hokkaido, Japan).

Protein and mRNA expression analyses

Whole-mount RNA in situ hybridization was performed as described (Saga et al., 1997). Whole-mount immunohistochemistry and simultaneous staining of *Mesp2* mRNA and Tbx6 protein were as previously described (Morimoto et al., 2005; Oginuma et al., 2008).

Chromatin immunoprecipitation (ChIP) assay

Embryonic tails were dissected along the anteroposterior axis into three parts using a tungsten needle. Somite part (s) corresponds to SIV to SII, anterior PSM (ap) is from SI to S-1, and posterior PSM (pp) corresponds to the region posterior to S-2. A total of 120 embryos were dissected, the samples treated with trypsin and dispersed cells counted (around 1×10^6 cells for each sample). Cells were fixed in 1% formaldehyde in PBS for 10 minutes at 37°C. The preparation of cell lysates and ChIP assay were performed using the Chromatin Immunoprecipitation Assay Kit (Upstate biology) according to the manufacturer's protocol. PCR primers used for ChIP assays were: LP286, 5′-AGACATCCAGGTACCTCGAGGTC-3′; LP287, 5′-CGG-GATAGACATCCAGGTACCCA-3′; and RP287, 5′-GGCTGGTGT-GACTCTGGGAAGCT-3′. LP286 and RP287 were used for detection of mutated P2PSME, whereas LP287 and RP287 were used for detection of wild-type P2PSME. As a positive control, the *Dll1* mesoderm (msd) enhancer was amplified using the following primers: LP259, 5′-CCCAACACAGATGATTCTGCCCAGTAACT-3′; and RP255, 5′-GCT-TTGTGTTGAGCATGCCATGAGCTGTA-3′. A sequence 22 kb from P2PSME was amplified by PCR as a negative control, using the following primers: LP285, 5′-GGTCTGTTTGCAGCTGATTCTGAA-3′; and RP286, 5′-CAGTTCTCACCTTGCTTCCATGT-3′.

Electromobility shift assay (EMSA)

The full-length *Tbx6* ORF was obtained from the pACT-Tbx6 construct, which was previously isolated from a yeast one-hybrid screen (Yasuhiko et al., 2006). After ligation to a 3×FLAG tag (Sigma), the tagged *Tbx6* insert was cloned into pCS2+ (Rupp et al., 1994). In vitro transcription/translation was then performed using the TNT In Vitro Translation Kit (Promega) according to the manufacturer's protocol. Oligonucleotide probes were labeled with DIG-11-ddUTP using recombinant TdT (Roche Diagnostics). Five microliters of crude in vitro translated product was subjected to EMSA. As a negative control, reticulocyte lysate without *Tbx6* template was used. The oligonucleotide probes are as follows (mutated nucleotides are indicated in lower case): SiteF, 5′-GCTAAATTACGGGTATATGGACCACAC-CTGTATCAGTCCC-3′; SiteG, 5′-CTGGGCTCTGTGGGTTTTGACA-CCTCTCTGCAACCTGGCA-3′; SiteGmut, 5′-CTGGGCTCTGTGG-GTTTTGAattCTCTCTGCAACCTGGCA-3′; SiteB, 5′-CCTTCGAGG-GGTCAGAATCCACACCTCTGCAAATGGGCCCGCTTT-3′; T1, 5′-CAAGTGCTGGTCTTGGCATCACACCTCTTTATTTGTTTCCATAC-3′; T2, 5′-GCAGAATCTGCAGAGGTGTCACTTCACACCTCTGTGG-CCTGGCT-3′; and T3, 5′-GCTCTCACAGCTGAGGTGTGAAGCG-ACACCTCCAGGCTCATAAG-3′.

EMSA was performed as described (Yasuhiko et al., 2006). Anti-Tbx6 antibody (3.5 μg) was added to the reaction to assess the specificity of the protein-DNA interaction. As a competitor, a 100-fold excess of unlabeled oligonucleotide corresponding to the probe was added to the reaction.

Transgenic assay

DNA fragments with and without mutations in conserved upstream sites were generated from an *Mesp2* genomic fragment using a standard PCR-based protocol. Each transgene comprised the *lacZ* reporter and a 6-kb genomic fragment upstream of the *Mesp2* first ATG, including P2PSME with and without mutated Tbx6 binding sites. The transgenes were injected into the male pronucleus of a fertilized egg as described (Hogan et al., 1994). Embryos recovered at E9.5-10.5 were analyzed for *lacZ* expression by X-Gal staining (Saga et al., 1992) and were subsequently examined for the presence of the transgene by PCR (Sasaki and Hogan, 1996).

Luciferase assay

The *Kpn*I-*Nco*I fragments (356 bp) corresponding to P2PSME, with and without mutations in the Tbx6 binding sites, were subcloned into the pGL3-Basic (Promega) vector to generate luciferase reporter constructs. The expression vectors for the proteins to be assessed were constructed in the same way as those used in the EMSA assays described above. The luciferase assay using COS-7 cells was conducted as described previously (Yasuhiko et al., 2006). Each assay was performed in triplicate and repeated at least twice.

RESULTS

Mutations in the Tbx6 binding site of the *Mesp2* enhancer result in the complete loss of *Mesp2* expression in the presomitic mesoderm

We have shown previously that nucleotide substitutions in two Tbx6 binding motifs in the *Mesp2* PSM enhancer (P2PSME) eliminate Tbx6 binding activity in vitro (Yasuhiko et al., 2006). To establish the function of these Tbx6 binding sites in vivo, we

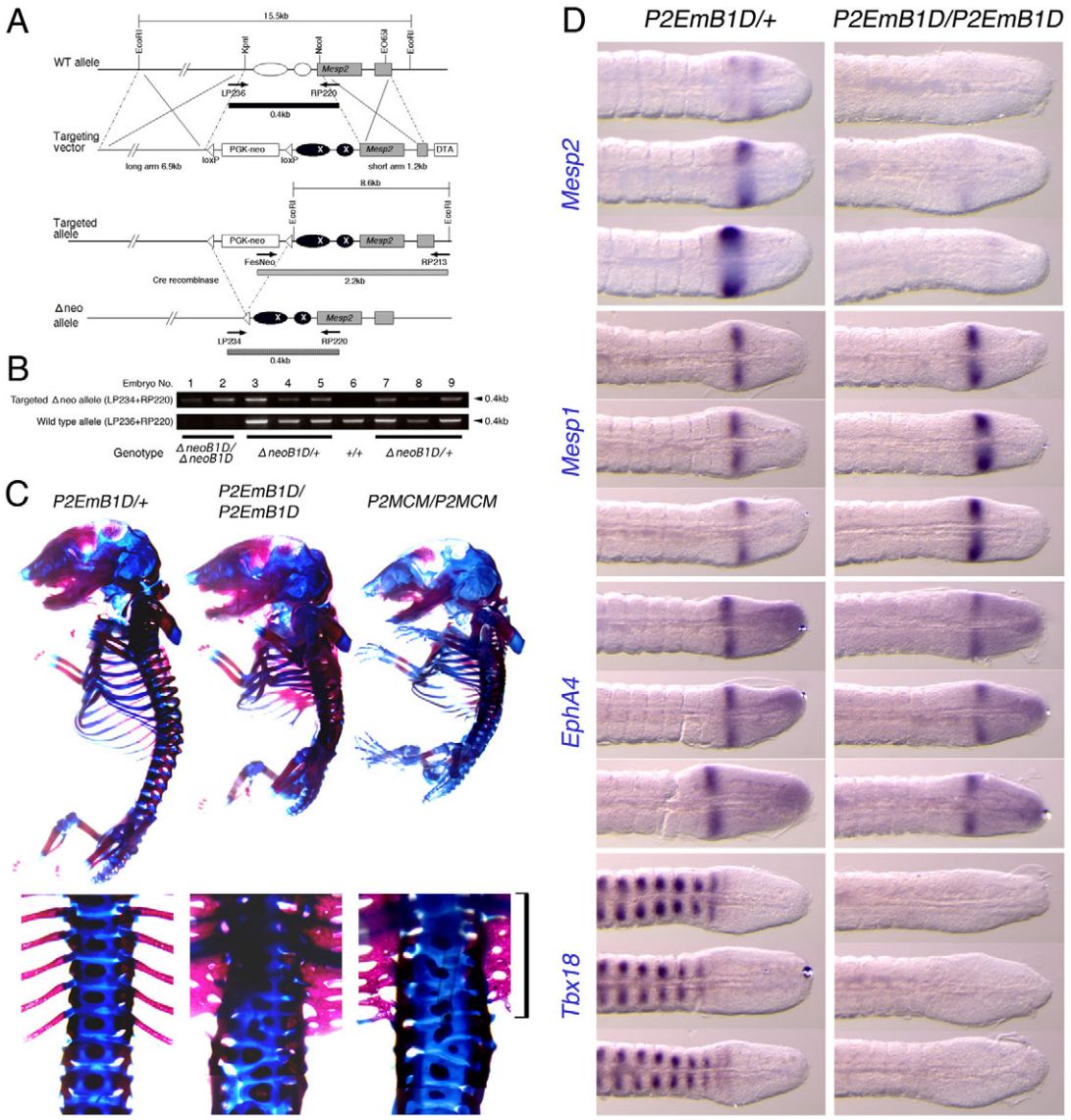

Fig. 1. Disruption of Tbx6 binding sites eliminates *Mesp2* expression. (**A**) Targeting strategy to generate the *Mesp2* enhancer knockout mouse (*P2EmB1D*). A DNA fragment containing mutated Tbx6 binding sites (black ovals with X) was substituted for the wild-type sequence (white ovals) by homologous recombination. The PGK-neoR selection marker was removed by the Cre-loxP system to obtain a Δneo allele. (**B**) PCR detection of homozygotes in the *P2EmB1D* intercross. (**C**) Impaired skeletal segmentation in the *Mesp2* enhancer knockout mouse. The *P2EmB1D/P2EmB1D* mouse exhibits severe skeletal malformation at E17.5 (centre) identical to that of the *Mesp2*-null mouse (*P2MCM/P2MCM*, right). Note the shortened spine with incompletely segmented vertebrae (upper panels) and fused ribs (bracket in lower panels). (**D**) Expression of *Mesp2* and the somite-specific genes *Mesp1*, *Epha4* and *Tbx18* in *P2EmB1D/+* (left column) and *P2EmB1D/P2EmB1D* (right column) embryos. *Mesp2* mRNA expression is eliminated in the *P2EmB1D/P2EmB1D* homozygotes. Wild-type (+/+) and heterozygote (*P2EmB1D/+*) embryos showed varying *Mesp2* expression patterns owing to its cyclic expression. *Mesp1* is upregulated and *Epha4* is not affected, whereas *Tbx18* is completely abolished in *P2EmB1D/P2EmB1D*.

introduced nucleotide substitutions into the mouse genome using a gene-targeting technique. These mutations disrupted two Tbx6 binding sites, denoted Site B and Site D, that were shown to be sufficient to activate *Mesp2* expression in vitro (Yasuhiko et al., 2006) (Fig. 1A). After the establishment of a neo*P2EmB1D* mouse line, the neoR cassette was removed (Δneo) by a cross with the deleter mouse line CAG-Cre. Interbreeding of the Δneo mutants gave rise to homozygotes (*P2EmB1D/P2EmB1D*) that retained a loxP site after neoR removal (Fig. 1B). This residual loxP site appears to have no effect on *Mesp2* expression or somitogenesis because another knock-in mouse, *P2EmCont*, in which wild-type P2PSME is knocked-in using the same strategy, had viable homozygous offspring without any morphological defects (data not shown).

The homozygous *P2EmB1D/P2EmB1D* embryos showed distinct skeletal defects (Fig. 1C) and perinatal lethality, features identical to the previously reported Δneo-type *Mesp2*-null mouse (Fig. 1C, *P2MCM/P2MCM*). As expected from the phenotype, *Mesp2* expression in *P2EmB1D/P2EmB1D* embryos was eliminated (Fig. 1D). Segmental borders were generated during an early stage of

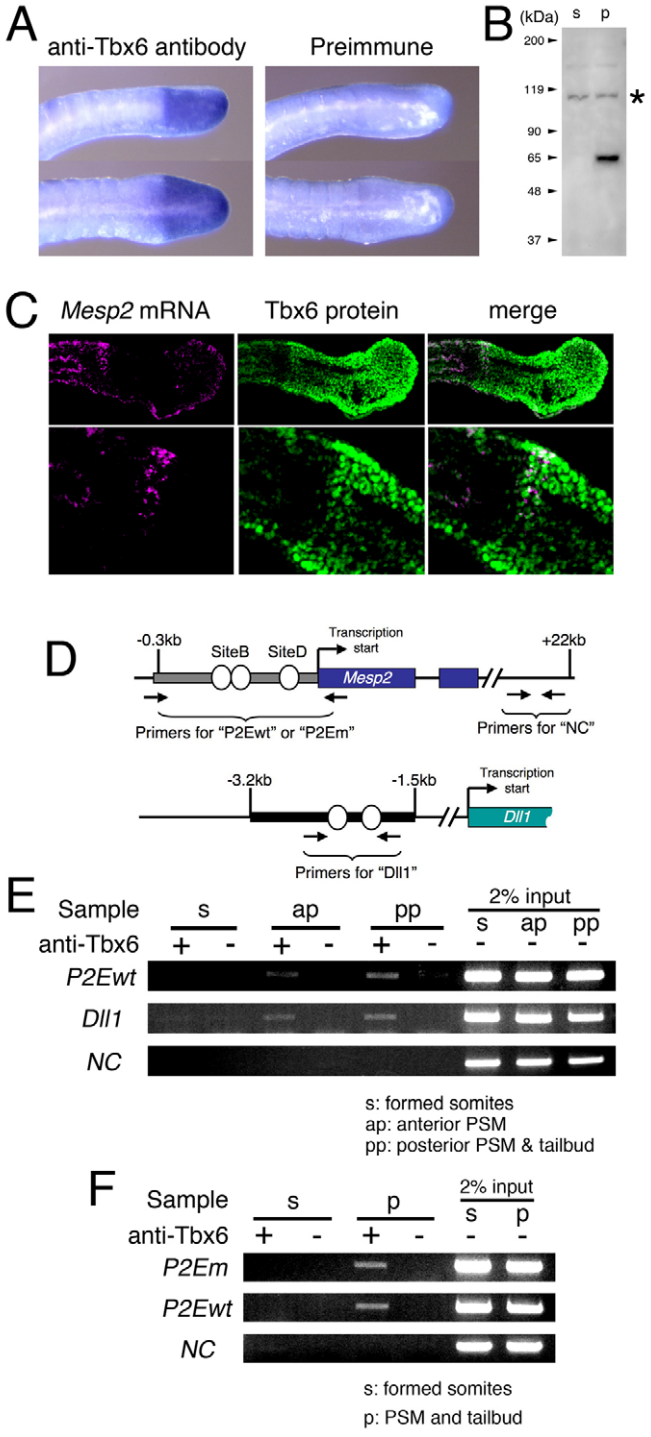

Fig. 2. Tbx6 binds to P2PSME in the PSM and tailbud. (**A**,**B**) Characterization of the anti-Tbx6 antibody produced in this study. (A) Whole-mount immunohistochemistry demonstrating the localization of Tbx6 protein in the mouse PSM and tailbud. (B) Western blot analysis showing that the anti-Tbx6 antibody detected a protein of expected molecular weight (58 kDa) in the PSM and tailbud (p) but not in formed somites (s). The asterisk indicates non-specific binding. (**C**) Double staining of *Mesp2* mRNA (purple) and Tbx6 protein (green) demonstrating the coexistence of both signals in the anterior-most part of the Tbx6-positive region (white in merged image). (**D**) Design of an in vivo technique for detecting Tbx6 binding to the P2PSME by ChIP. Arrows represent primers for the ChIP assay for the *Mesp2* and *Dll1* genes. *Dll1* is known to be downstream of Tbx6 and was therefore used as a positive control. Gray and black boxes represent the P2PSME and *Dll1* mesoderm (msd) enhancers, respectively. White ovals indicate Tbx6 binding sites. P2Em and P2Ewt, mutated and wild-type P2PSME regions, respectively; NC, unrelated sequence as negative control. (**E**) Tbx6 associates with P2PSME in the anterior and posterior PSM. (**F**) The association of Tbx6 with mutated P2PSME as detected by ChIP assay. Mutated and wild-type P2PSME regions were differentially detected by PCR with different sets of primers in the tails of E10.5 embryos obtained from the crossing of *P2EmB1D*/+ and ICR mice.

somitogenesis (Fig. 1D, right-hand panels). However, the borders were unlikely to be maintained because the vertebral bodies were fused along the anteroposterior axis at later developmental stages (Fig. 1C).

To further characterize the phenotypes in these embryos, we first examined the expression of *Mesp1*, which is known to be upregulated and to partially rescue somitogenesis in the absence of *Mesp2* (Morimoto et al., 2006; Takahashi et al., 2007). *Mesp1* expression was upregulated in the *P2EmB1D/P2EmB1D* embryo, but its expression domain was broader than normal (Fig. 1D). *Epha4*, which is required for proper border formation, was expressed normally. However, *Tbx18*, which is implicated in the maintenance of segmental border and somite patterning (Bussen et al., 2004), was not expressed (Fig. 1D). These gene expression patterns were similar to those reported for the Δneo-type *Mesp2*-null mouse (Morimoto et al., 2006; Takahashi et al., 2007). These results confirmed that the Tbx6 binding sites are bona fide enhancer elements required for *Mesp2* expression.

Tbx6 binds the *Mesp2* PSM enhancer in vivo

The Tbx6 protein is normally broadly distributed in the PSM and tailbud (White and Chapman, 2005), whereas *Mesp2* is expressed only in the anterior PSM (Saga et al., 1997). This discrepancy between the Tbx6 and *Mesp2* expression patterns prompted us to investigate whether Tbx6 actually binds to the *Mesp2* enhancer in vivo. We raised an anti-Tbx6 antibody using two different antigens: an N-terminal portion of Tbx6 and an internal portion. The internal antigen yielded an antibody with good specificity and sensitivity. Embryo whole-mount immunohistochemistry confirmed the previously reported distinct Tbx6 staining pattern in the PSM and tailbud (Fig. 2A) (White and Chapman, 2005). Western blot analyses further revealed that this antibody identifies a single band of approximately 58 kDa in cell lysates prepared from the posterior region (PSM and tailbud), but not from the anterior region (formed somite), of E11.5 tails (Fig. 2B). We also performed double staining of *Mesp2* mRNA and Tbx6 protein and confirmed colocalization only in the anterior-most region of the PSM (Fig. 2C).

For ChIP assays, we dissected E11.5 embryo tails into three regions: the tailbud and posterior PSM (pp), the anterior PSM and newly formed somites (ap), and formed somites (s). Protein-DNA complexes were prepared from each pool and used in ChIP assays, which revealed that Tbx6 binds to the *Mesp2* PSM enhancer in the ap and pp regions, but not in the s region, which is consistent with the expression pattern of Tbx6 (Fig. 2E). These results indicate that Tbx6 binds to the P2PSME uniformly in its expression domain, suggesting that Tbx6 alone cannot activate *Mesp2* in the posterior PSM where it binds. *Dll1* is known to be a downstream target of Tbx6 and putative binding sites have been identified in its mesoderm

(msd) enhancer (White and Chapman, 2005). ChIP assays using the putative *Dll1* msd enhancer (Fig. 2E, column Dll1) revealed that Tbx6 also binds to the *Dll1* enhancer in both the ap and pp regions, which is consistent with the expression pattern of *Dll1*. In all cases, the negative control (PCR amplification of an unrelated sequence in the mouse genome) gave no signal in ChIP assays with the anti-Tbx6 antibody (Fig. 2E,F, column NC). Thus, these results confirm our previous finding that Tbx6 binding is required for *Mesp2* expression, but is not sufficient for full transcriptional activation.

Mutated P2PSME contains Tbx6 binding sites that are inactive in vivo

We next applied the ChIP assay system to confirm that the phenotype of our enhancer-specific knockout mouse was due to the lack of Tbx6 binding in the *Mesp2* enhancer region. We performed ChIP assays using the tails of *P2EmB1D* heterozygous embryos and specific primer sets in order to distinguish the mutated DNA fragment from its wild-type counterpart, expecting that Tbx6 would not bind to the mutated enhancer. Surprisingly, mutated P2PSME, which has no PSM-specific transcriptional activity (Fig. 1), gave rise to a band that co-precipitated with the anti-Tbx6 antibody. This indicated that Tbx6 still binds to the mutated PSME in vivo (Fig. 2F). To identify the Tbx6 binding site within the mutated P2PSME, we re-examined this region for a consensus Tbx6 binding sequence (White and Chapman, 2005) and found two additional candidate sites, denoted Site F and Site G, in and upstream of P2PSME (Fig. 3A). EMSA demonstrated that Site G was strongly associated with Tbx6 in vitro (Fig. 3B).

The number and spatial organization of the T-box binding sites are important for initiating *Mesp2* transcription via Notch signaling

We reported previously that the simultaneous mutation of two Tbx6 binding sites, Site B and Site D, eliminates PSM-specific activation of a reporter gene by P2PSME in transgenic embryos (Yasuhiko et al., 2006). To confirm this finding and also investigate the possible involvement of the new Tbx6 binding site, Site G, in enhancer activity, we generated a series of reporter constructs with P2PSME harboring serial mutations in the Tbx6 binding sites. We tested two types of reporter assay: a luciferase assay using cultured cells, and transgenic analyses. In the luciferase assay, the loss of any single Tbx6 binding site among Sites B, D and G, caused a 10-fold reduction in Tbx6-dependent and Tbx6 plus Notch signaling-dependent reporter activation (Fig. 3C, right). Conversely, expression of a *lacZ* reporter in transgenic embryos was not markedly affected by the loss of any individual Tbx6 binding site (Fig. 3C, left). These results suggested that each Tbx6 binding site contributes equally to P2PSME activity, but that the loss of a single site is not sufficient to disrupt the in vivo function of P2PSME.

We next examined the effects of systematically removing multiple Tbx6 binding sites. Removal of two Tbx6 binding sites from P2PSME resulted in a further decrease in luciferase reporter activity (Fig. 3C, lane P2EmDG, and Fig. 3D). *lacZ* expression in transgenic embryos was also diminished, both in intensity and frequency. Out of nine transgene-positive embryos, only one showed weak *lacZ* expression with the P2EmB1 reporter, which has two intact Tbx6 binding sites (Fig. 3D, left). When three out of four Tbx6 binding sites were eliminated, the synergistic effects of Tbx6 and Notch signaling on P2PSME activation were no longer observed and mutants resembled P2EmB1DG, which has lost Tbx6 binding capability at all four sites (Fig. 3D, right). In transgenic embryos, *lacZ* expression was not activated by any single Tbx6 binding site (Fig. 3D, left, P2EmB1D). These results strongly suggest that the PSM-specific expression of *Mesp2* requires at least two Tbx6 binding sites in P2PSME. Notably, the P2PSME reporters with two intact Tbx6 binding sites (P2EmDG, P2EmB1, P2EmB2D, P2EmB2G) showed variable levels of activity in the luciferase assay. This finding contrasts with the uniform reporter activity found with either one or three mutated Tbx6 binding sites (Fig. 3C,D). P2EmDG, with two Tbx6 binding sites in Site B intact, displayed a more than 2-fold stronger activity than P2EmB2G, which harbors single Tbx6 binding sites within Site B and Site D. P2EmB2G activated the luciferase reporter at levels comparable to those of reporters with a single Tbx6 binding site and showed no synergistic activation when Notch signaling was applied (Fig. 3D). Taken together, these data indicate that the four Tbx6 binding sites have equal importance in regulating P2PSME activity, and at least two neighboring sites are required for the Notch signaling-dependent induction of *Mesp2* expression.

The medaka *mespb* PSM enhancer regulates *Mesp2* expression and normal somite formation in the mouse embryo

mespb, the zebrafish homolog of *Mesp2*, shows a similar expression pattern to mouse *Mesp2* during embryogenesis and we speculated that it might exert a similar function in the mouse (Nomura-Kitabayashi et al., 2002). We have previously identified the PSM-specific enhancer of medaka *mespb*, which contains T-box binding sites. Two of these sites, T1 and T2, are important for PSM-specific *mespb* expression (Terasaki et al., 2006) (Fig. 4A). These data suggest that the T-box-protein-dependent expression mechanism is evolutionally conserved between mammals and teleosts (zebrafish, medaka). We demonstrated that zebrafish Tbx24, a T-box protein that is homologous to mouse Tbx6 and is responsible for the *fused somite* (*fss*) mutant phenotype, binds to the medaka *mespb* PSME (Fig. 4B). A sequence comparison revealed three putative T-box binding sites in the medaka *mespb* PSME (Fig. 4A). Two of these had the ability to bind two Tbx24 molecules each, whereas in the mouse P2PSME, only Site B can bind two Tbx6 molecules (Fig. 4B).

To more directly demonstrate the evolutionary conservation of this regulatory mechanism, we generated a knock-in mouse with a medaka *mespb* upstream sequence inserted in place of the endogenous *Mesp2* PSME. For this purpose, we substituted the 356-bp sequence upstream of the *Mesp2* first ATG with 2.8 kb of sequence upstream of the *mespb* first ATG, generating a *medakaP2* mouse (Fig. 4C). Heterozygous mice (*medakaP2/+*) were viable and appeared normal (data not shown). Homozygous mice (*medakaP2/medakaP2*) were also viable and showed no physical malformations (Fig. 4D). In skeletal preparations, we observed that *medakaP2* homozygous fetuses were indistinguishable from heterozygous or wild-type littermates (Fig. 4E), indicating that the PSMEs of medaka *mespb* and mouse *Mesp2* are functionally equivalent, despite some differences in their structural features.

DISCUSSION

The activation of *Mesp2* expression requires at least two Tbx6 binding sites in P2PSME

In our current study, we have shown that Tbx6 binding sites are fundamentally important for P2PSME function and that P2PSME is necessary and sufficient for *Mesp2* expression during somite formation in mouse embryogenesis. However, ChIP assays revealed that Tbx6 binds to P2PSME not only in *Mesp2*-expressing cells, but also in non-expressing cells such as those in the tailbud and posterior

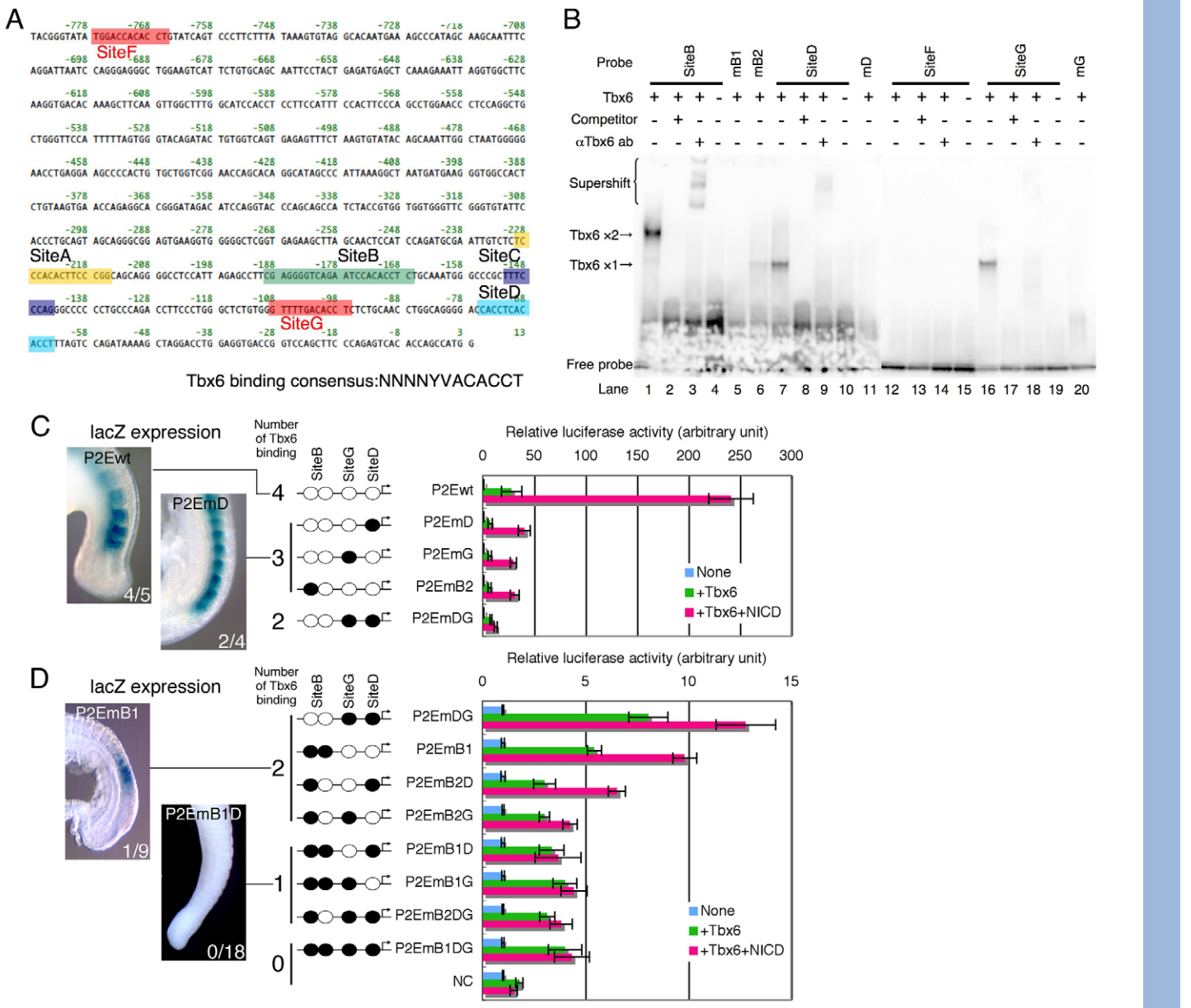

Fig. 3. Multiple Tbx6 binding is required for Mesp2 activation. (**A**) The sequence of the mouse *Mesp2* enhancer region that contains four presumptive Tbx6 binding sites (Sites B, D, F and G). Sites A and C are presumptive RBPJ-κ binding sites (Yasuhiko et al., 2006). The Tbx6 consensus binding site was originally reported by White and Chapman (White and Chapman, 2005). (**B**) Site G, but not Site F, binds to Tbx6 in an electromobility shift assay (EMSA). Site G produced a bandshift indicating a single bound Tbx6 molecule (lane 16), whereas Site B produced two bands (lane 1). Mutated oligonucleotide probes mB1, mD and mG produced no shifted bands (lanes 5, 11 and 20, respectively). The mB2 probe showed a single shifted band, implying the loss of one Tbx6 binding site in Site B (lane 6). (**C**,**D**) Luciferase reporter assays were conducted using several mutated enhancer elements. Luciferase activity was measured after transfection of reporter constructs along with an empty vector (None), Tbx6 expression vector (+Tbx6), or both Tbx6 and Notch intracellular domain expression vectors (+Tbx6 +NICD). Each reporter construct is presented schematically to the left of each graph. Black oval, mutated Tbx6 binding site; white oval, wild-type Tbx6 binding site; arrow, transcription start site. The number of wild-type Tbx6 binding sites is also indicated (number of Tbx6 binding: C, 4 to 2; D, 2 to 0). To the left are representative images of *lacZ* staining in transgenic embryos with P2PSME-*lacZ* reporters bearing the indicated enhancers. The number of *lacZ*-positive/transgene-positive embryos is indicated. The results of a consecutive series of reporter assays, as described in C, are shown in D, but on a different scale owing to the steep declines in activity. The P2EmDG lane represents the same data in both C and D. Each luciferase assay was performed in triplicate in at least three independent experiments. Error bars represent s.d.

PSM (Fig. 2E). This indicates that Tbx6 binding alone is not sufficient to activate *Mesp2* expression. Previously, we showed in vitro that *Mesp2* was activated weakly, if at all, by Tbx6 alone, but rigorously by a coexisting Notch signal (Yasuhiko et al., 2006). Taken together, these data suggest that it is highly likely that the restricted expression pattern of *Mesp2* in the anterior PSM is regulated by a combination of Tbx6 and Notch signaling in vivo. Similarly, Tbx6 activates *Dll1* together with Wnt signaling (Hofmann et al., 2004) and activates *Ripply* in cooperation with Mesp2 (Hitachi et al., 2008). Although the molecular mechanisms

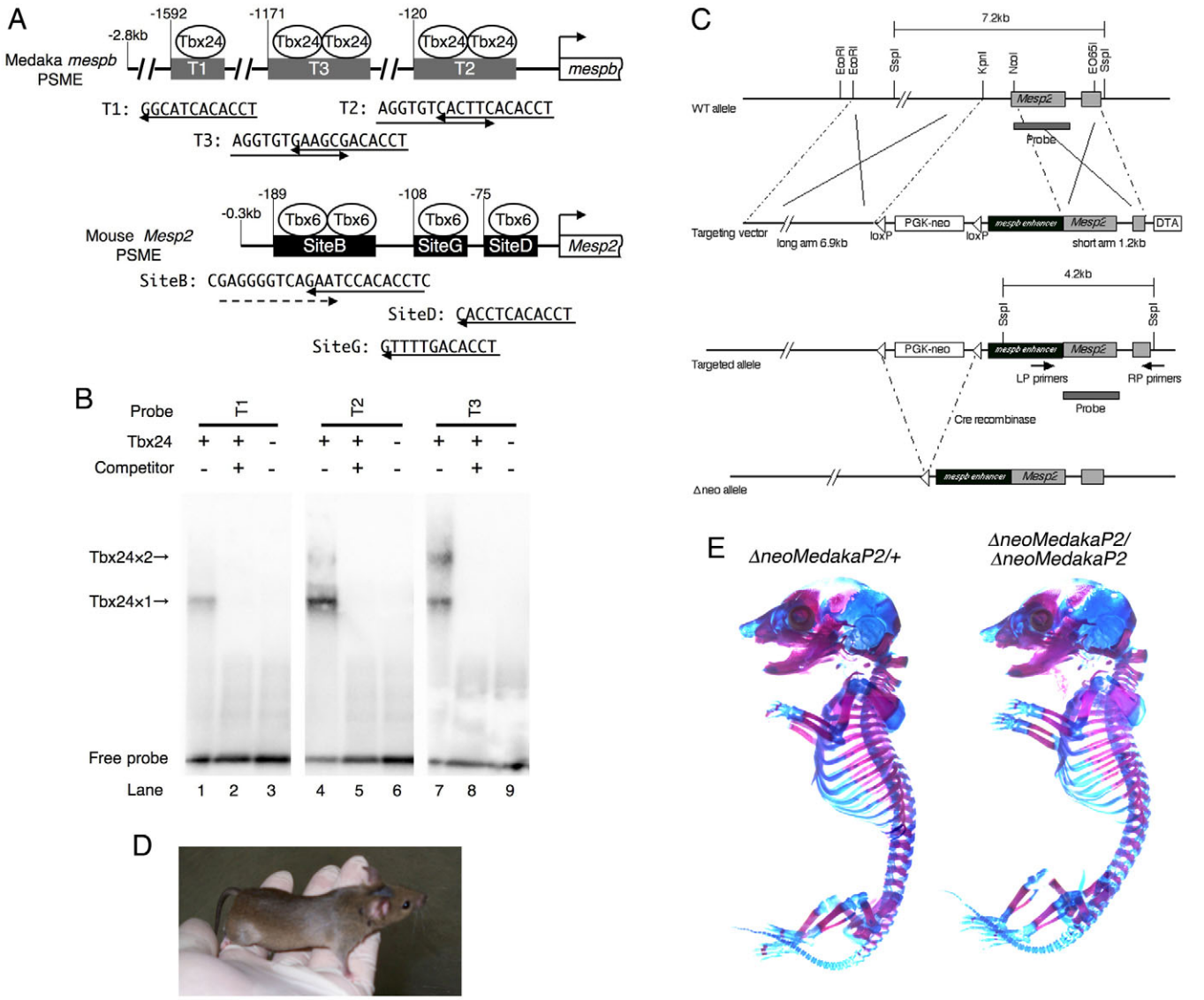

Fig. 4. The medaka *mespb* PSM enhancer is functionally equivalent to its counterpart in the mouse. (**A**) A comparison of the medaka *mespb* and mouse *Mesp2* PSME regions. Black and gray boxes represent presumptive T-box binding sites. The numbers above the boxes represent the nucleotide positions from the first ATG. The nucleotide sequences of the putative T-box binding sequences are shown beneath. Consensus Tbx6 binding sequences and their directions are indicated by arrows. The dashed arrow in Site B of the *Mesp2* PSME depicts an incomplete Tbx6 binding sequence that only binds to Tbx6 if an adjoining complete Tbx6 binding sequence is present. The T-box proteins that might bind to these sequences are indicated. (**B**) EMSA analysis of the T-box binding sites in the medaka *mespb* PSME. T-box binding site T1 associates with a single Tbx24 molecule and T2 and T3 with two Tbx24 molecules, which is consistent with their nucleotide sequences as shown in A. (**C**) The targeting strategy used to generate the medaka *mespb* PSME knock-in mouse (*medakaP2*). A 2.8-kb fragment of *mespb* genomic DNA that is required for PSM-specific *mespb* expression was substituted for *Mesp2* PSME by homologous recombination. The neoR selection marker was removed by recombination using the Cre-loxP system. (**D**) *medakaP2* homozygotes are viable and have normal external features. (**E**) Homozygotes are indistinguishable from heterozygotes and wild-type littermates in skeletal preparations.

by which Tbx6 regulates its target genes together with various partners remain elusive, it is possible that the number and spatial organization of Tbx6 binding sites facilitate the response of P2PSME to Notch signaling.

In total, there are four Tbx6 binding sequences in this region: two palindrome-like sequences in Site B and one each in Sites D and G. Importantly, the P2PSME reporters with only one intact Tbx6 binding site were inactive in both the luciferase assay and the transgenic analyses (Fig. 3D), suggesting that a single P2PSME-bound Tbx6 molecule might not act as a mediator of Notch signaling in the regulatory mechanism controlling *Mesp2* expression. This is consistent with the observation that Site G fails to activate *Mesp2* expression by itself in the *P2EmB1D* mouse.

The loss of two or more of the four Tbx6 binding sites greatly diminishes P2PSME activity in both luciferase and transgenic assays (Fig. 3D). Interestingly, the reporters with two intact Tbx6 binding sites showed varied levels of activity depending upon the position of the intact sites. Two intact Tbx6 binding sites in Site B resulted in the highest reporter activity (Fig. 3D). These data indicate that Site B may be of predominant importance in the function of P2PSME,

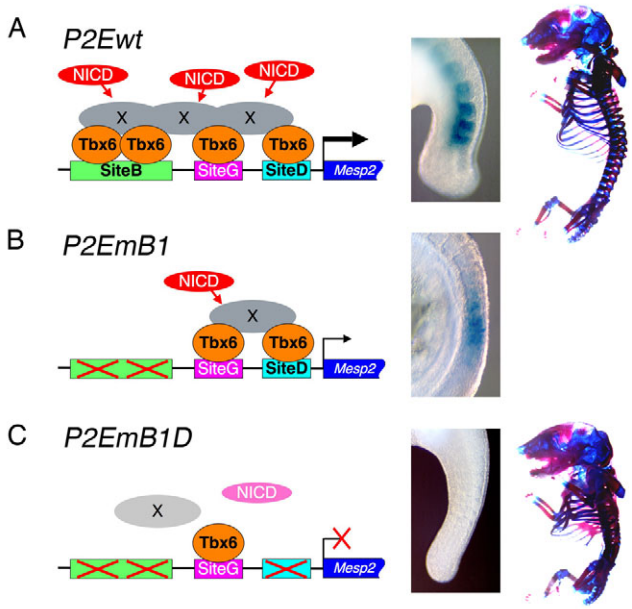

Fig. 5. Putative mechanism for the Tbx6-mediated regulation of Mesp genes. (**A**) Tbx6 activates *Mesp2* expression through multiple Tbx6 binding sites. Notch signaling (NICD, red ovals) activates *Mesp2* expression via factor X (gray ovals), which recognizes two neighboring Tbx6 binding sites in P2PSME. (Left) Schematic description of the Tbx6-dependent activation of *Mesp2*. (Middle column) *lacZ* expression in the P2Ewt transgenic embryo. (Right) Normal skeletal formation in the heterozygous fetus of a *P2EmB1D* mouse. (**B**) Mutation in Site B results in decreased expression of *Mesp2*. (**C**) A single Tbx6 binding site is unable to activate *Mesp2* expression, presumably owing to an inability to respond to Notch signaling.

implying that its two neighboring Tbx6 binding sites play a central role in regulating the activation of *Mesp2*. The binding of Tbx6 to one of the two binding sites in Site B depends on the presence of another Tbx6 molecule binding to this site (Yasuhiko et al., 2006). This property might be related to the unique palindrome-like sequence of this site. Although several T-box binding sites have been identified in the upstream region of other Tbx6-downstream genes, such as *Dll1* (Hofmann et al., 2004) and *Msgn1* (Wittler et al., 2007), the palindrome-like site has thus far been found only in the PSME of *Mesp2* and its medaka ortholog *mespb* (Fig. 4A). It is therefore possible that two neighboring Tbx6 molecules on the palindrome-like site are specifically recognized by as yet unidentified factor(s) (Fig. 5, 'X') that together with Tbx6 constitutes an RBPJ-κ (Rbpj)-independent Notch signaling machinery [disruption of potential RBPJ-κ binding sites does not affect P2PSME activity in transgenic embryos (Yasuhiko et al., 2006)]. Further analyses of *Mesp2* PSME might shed light on these novel regulatory mechanisms that operate during development.

Mutations that removed any one of the Tbx6 binding sites in P2PSME, regardless of which, diminished luciferase reporter activity by the same amount (Fig. 3C), suggesting that each Tbx6 binding site contributes equally to *Mesp2* expression in vitro. In vivo, by contrast, the mutation of a single Tbx6 binding site did not seem to affect PSM-specific gene expression (Fig. 3C). Taken together, these results indicate that the multiple Tbx6 binding sites confer a functional robustness to P2PSME that ensures proper *Mesp2* expression during embryogenesis.

An evolutionally conserved mechanism regulating Mesp expression through multiple T-box binding sites

We previously found that the deletion of two T-box binding sites in the *mespb* PSME greatly reduced its PSM-specific enhancer activity in transgenic medaka embryos (Terasaki et al., 2006), similar to our findings in transgenic mouse embryos. The medaka *mespb* PSME harbors three T-box binding sites (T1-T3), which is similar to the complement of the mouse *Mesp2* PSME (Fig. 4A). However, the total length of the PSME is very different between mouse *Mesp2* and medaka *mespb* (356 bp versus 2.8 kb, respectively) (Terasaki et al., 2006). The number of T-box proteins that bind to the medaka and mouse PSMEs is also different (Fig. 4A,B), and the distance between each element is greater in the *mespb* PSME than in its mouse counterpart.

We have demonstrated, however, that the medaka *mespb* PSME is functionally equivalent to the mouse *Mesp2* PSME. In our transgenic assay, a mutation in the double T-box binding site (Site B in mouse and Site T2 in medaka) had the most profound effect upon PSME activity. Consistent with these results, deletion of medaka Site T1 (harboring a single T-box binding sequence) did not affect reporter gene expression. However, deletion of one of the sites within the double T-box binding sequence (T2) caused a 50% decrease in reporter expression (Terasaki et al., 2006), again demonstrating the importance of the binding to the double T-box site for PSM enhancer function.

In the teleost fish, zebrafish, the T-box transcription factor Tbx24 was identified as responsible for the fused somite (*fss*) mutant phenotype. Tbx24 has a T-box domain that is homologous to that of mouse Tbx6 (Nikaido et al., 2002). The segmentation of somites and expression of *mespb* are eliminated in the *fss* mutant (Sawada et al., 2000), implying that *mespb* is a downstream target of Tbx24, similar to the relationship between *Mesp2* and Tbx6 in mice. However, *fss* mutant fish are viable and fertile (van Eeden et al., 1996), whereas *Tbx6*-null mouse embryos fail to form a mesoderm and die early in development (Chapman and Papaioannou, 1998). This difference might be due to the presence in zebrafish of a *Tbx6* counterpart gene, *spadetail*, which supports paraxial mesoderm formation. Despite this difference, our data clearly demonstrate that the mechanism regulating the PSM-specific expression of *Mesp2* and *mespb* is evolutionarily well conserved between fish and mice.

We thank Hiroyuki Takeda (University of Tokyo) for providing Tbx24 cDNA clones and Mariko Ikumi, Eriko Ikeno and Shunsuke Matsusaka for technical assistance. This work was supported by a grant-in-aid for scientific research from the Ministry of Education, Culture, Sports, Science and Technology, Japan, a grant for Research on Risk on Chemical Substances (H20-004) from the Ministry of Health, Labor and Welfare of Japan, and a grant from the NIG Cooperative Research Program (2007-B66).

References

Bussen, M., Petry, M., Schuster-Gossler, K., Leitges, M., Gossler, A. and Kispert, A. (2004). The T-box transcription factor Tbx18 maintains the separation of anterior and posterior somite compartments. *Genes Dev.* **18**, 1209-1221.

Chapman, D. L. and Papaioannou, V. E. (1998). Three neural tubes in mouse embryos with mutations in the T-box gene Tbx6. *Nature* **391**, 695-697.

Chapman, D. L., Agulnik, I., Hancock, S., Silver, L. M. and Papaioannou, V. E. (1996). Tbx6, a mouse T-Box gene implicated in paraxial mesoderm formation at gastrulation. *Dev. Biol.* **180**, 534-542.

Delfini, M. C., Dubrulle, J., Malapert, P., Chal, J. and Pourquie, O. (2005). Control of the segmentation process by graded MAPK/ERK activation in the chick embryo. *Proc. Natl. Acad. Sci. USA* **102**, 11343-11348.

Dunty, W. C., Jr, Biris, K. K., Chalamalasetty, R. B., Taketo, M. M., Lewandoski, M. and Yamaguchi, T. P. (2008). Wnt3a/β-catenin signaling controls posterior body development by coordinating mesoderm formation and segmentation. *Development* **135**, 85-94.

Galceran, J., Sustmann, C., Hsu, S. C., Folberth, S. and Grosschedl, R. (2004). LEF1-mediated regulation of Delta-like1 links Wnt and Notch signaling in somitogenesis. *Genes Dev.* **18**, 2718-2723.
Haraguchi, S., Kitajima, S., Takagi, A., Takeda, H., Inoue, T. and Saga, Y. (2001). Transcriptional regulation of Mesp1 and Mesp2 genes: differential usage of enhancers during development. *Mech. Dev.* **108**, 59-69.
Hitachi, K., Kondow, A., Danno, H., Inui, M., Uchiyama, H. and Asashima, M. (2008). Tbx6, Thylacine1, and E47 synergistically activate bowline expression in Xenopus somitogenesis. *Dev. Biol.* **313**, 816-828.
Hofmann, M., Schuster-Gossler, K., Watabe-Rudolph, M., Aulehla, A., Herrmann, B. G. and Gossler, A. (2004). WNT signaling, in synergy with T/TBX6, controls Notch signaling by regulating Dll1 expression in the presomitic mesoderm of mouse embryos. *Genes Dev.* **18**, 2712-2717.
Hogan, B., Beddington, R., Costantini, F. and Lacy, E. (1994). *Manipulating the Mouse Embryo: a Laboratory Manual*. Cold Spring Harbor, NY: Cold Spring Harbor Laboratory Press.
Moreno, T. A. and Kintner, C. (2004). Regulation of segmental patterning by retinoic acid signaling during Xenopus somitogenesis. *Dev. Cell* **6**, 205-218.
Morimoto, M., Takahashi, Y., Endo, M. and Saga, Y. (2005). The Mesp2 transcription factor establishes segmental borders by suppressing Notch activity. *Nature* **435**, 354-359.
Morimoto, M., Kiso, M., Sasaki, N. and Saga, Y. (2006). Cooperative Mesp activity is required for normal somitogenesis along the anterior-posterior axis. *Dev. Biol.* **300**, 687-698.
Nikaido, M., Kawakami, A., Sawada, A., Furutani-Seiki, M., Takeda, H. and Araki, K. (2002). Tbx24, encoding a T-box protein, is mutated in the zebrafish somite-segmentation mutant fused somites. *Nat. Genet.* **31**, 195-199.
Nomura-Kitabayashi, A., Takahashi, Y., Kitajima, S., Inoue, T., Takeda, H. and Saga, Y. (2002). Hypomorphic Mesp allele distinguishes establishment of rostrocaudal polarity and segment border formation in somitogenesis. *Development* **129**, 2473-2481.
Oginuma, M., Niwa, Y., Chapman, D. L. and Saga, Y. (2008). Mesp2 and Tbx6 cooperatively create periodic patterns coupled with the clock machinery during mouse somitogenesis. *Development* **35**, 2555-2562.
Rupp, R. A., Snider, L. and Weintraub, H. (1994). Xenopus embryos regulate the nuclear localization of XMyoD. *Genes Dev.* **8**, 1311-1323.
Saga, Y. and Takeda, H. (2001). The making of the somite: molecular events in vertebrate segmentation. *Nat. Rev. Genet.* **2**, 835-845.
Saga, Y., Yagi, T., Ikawa, Y., Sakakura, T. and Aizawa, S. (1992). Mice develop normally without tenascin. *Genes Dev.* **6**, 1821-1831.
Saga, Y., Hata, N., Koseki, H. and Taketo, M. M. (1997). Mesp2: a novel mouse gene expressed in the presegmented mesoderm and essential for segmentation initiation. *Genes Dev.* **11**, 1827-1839.
Sasaki, H. and Hogan, B. L. (1996). Enhancer analysis of the mouse HNF-3 beta gene: regulatory elements for node/notochord and floor plate are independent and consist of multiple sub-elements. *Genes Cells* **1**, 59-72.
Sawada, A., Fritz, A., Jiang, Y. J., Yamamoto, A., Yamasu, K., Kuroiwa, A., Saga, Y. and Takeda, H. (2000). Zebrafish Mesp family genes, mesp-a and mesp-b are segmentally expressed in the presomitic mesoderm, and Mesp-b confers the anterior identity to the developing somites. *Development* **127**, 1691-1702.
Takahashi, Y., Koizumi, K., Takagi, A., Kitajima, S., Inoue, T., Koseki, H. and Saga, Y. (2000). Mesp2 initiates somite segmentation through the Notch signalling pathway. *Nat. Genet.* **25**, 390-396.
Takahashi, Y., Inoue, T., Gossler, A. and Saga, Y. (2003). Feedback loops comprising Dll1, Dll3 and Mesp2, and differential involvement of Psen1 are essential for rostrocaudal patterning of somites. *Development* **130**, 4259-4268.
Takahashi, Y., Yasuhiko, Y., Kitajima, S., Kanno, J. and Saga, Y. (2007). Appropriate suppression of Notch signaling by Mesp factors is essential for stripe pattern formation leading to segment boundary formation. *Dev. Biol.* **304**. 593-603.
Terasaki, H., Murakami, R., Yasuhiko, Y., Shin, I. T., Kohara, Y., Saga, Y. and Takeda, H. (2006). Transgenic analysis of the medaka mesp-b enhancer in somitogenesis. *Dev. Growth Differ.* **48**, 153-168.
van Eeden, F. J., Granato, M., Schach, U., Brand, M., Furutani-Seiki, M., Haffter, P., Hammerschmidt, M., Heisenberg, C. P., Jiang, Y. J., Kane, D. A. et al. (1996). Mutations affecting somite formation and patterning in the zebrafish, Danio rerio. *Development* **123**, 153-164.
White, P. H. and Chapman, D. L. (2005). Dll1 is a downstream target of Tbx6 in the paraxial mesoderm. *Genesis* **42**, 193-202.
Wittler, L., Shin, E. H., Grote, P., Kispert, A., Beckers, A., Gossler, A., Werber, M. and Herrmann, B. G. (2007). Expression of Msgn1 in the presomitic mesoderm is controlled by synergism of WNT signalling and Tbx6. *EMBO Rep.* **8**, 784-789.
Yagi, T., Tokunaga, T., Furuta, Y., Nada, S., Yoshida, M., Tsukada, T., Saga, Y., Takeda, N., Ikawa, Y. and Aizawa, S. (1993). A novel ES cell line, TT2, with high germline-differentiating potency. *Anal. Biochem.* **214**, 70-76.
Yasuhiko, Y., Haraguchi, S., Kitajima, S., Takahashi, Y., Kanno, J. and Saga, Y. (2006). Tbx6-mediated Notch signaling controls somite-specific Mesp2 expression. *Proc. Natl. Acad. Sci. USA* **103**, 3651-3656.